Continuous-Domain Real-Time Distributed ADMM Algorithm for Aggregator Scheduling and Voltage Stability in Distribution Network

Towfiq Rahman, Ying Xu and Zhihua Qu

***Abstract*—With an increase in the number of electric vehicles (EVs) and battery storage systems (BSSs), there are major challenges in the distribution grid to maintain a scaling control structure. Also, with the vehicle to grid (V2G) technology, EVs can now inject power into the grid for voltage regulation. This paper proposes a new distributed real-time alternating direction method of multipliers (ADMM) technique to control EVs and BSSs for voltage regulation while maximizing their utility function. More specifically, a continuous-domain real-time optimization and control algorithm is developed in closed form which exchanges relevant information among the neighboring nodes through the communication network, optimizes a combined convex objective of EVs and BSSs welfare and voltage regulation with power flow equations as constraints. Convergence analysis is provided using the Lyapunov direct approach and simulation results are included to illustrate the effectiveness of the proposed scheme.**

Index Terms - Real-time Distributed Optimization, Aggregators, Electric Vehicle, Battery Storage Systems, ADMM, Lyapunov Direct Method.

***Note to Practitioners*—This paper is motivated by the problems an electric distribution system is facing today due to the penetration of electric vehicles and battery storage systems. The presence of a large number of EVs and BSSs is causing a substantial degradation of the quality and reliability of the power grid. Despite the adverse effects, EVs and BSSs can be controlled and used as a power source to benefit the grid. Also, this control of EVs and BSS cannot be done by a centralized body since that would be non-scalable and would require huge communication bandwidth. To tackle this ever scaling problem, this paper develops a continuous domain multi-agent distributed algorithm to control the EVs and BSSs and utilize them to maintain the grid voltage within the normal operating range while also satisfying the consumers by maximizing their welfare. The algorithm was developed in the continuous domain since in most of the other algorithms which are iterative and in discrete time, the accuracy of the optimal solution greatly depends on the sampling time, thus it is not robust to changes that are prevalent with distributed energy resources like EVs and BSSs.**

NOMENCLATURE

Functions

f_i	Objective function of agent i
H_i	DSO penalty function
J_i	Objective function of node/bus i
W_i	EV and BSS owner welfare function

Power System Variables

Γ_i	Parent node of node i
$B_{\Gamma_i i}$	Susceptance on the line between node Γ_i and i
I_i	Current flow between parent node Γ_i and node i
$jQ_{\Gamma_i i}$	Reactive power flow from parent node Γ_i to node i
jQ_{d_i}	Reactive load demand at node i
jq_i	Aggregated reactive power EV and BSS injection at node i
l_i	Square of the Current flow between parent node Γ_i and node i
$P_{\Gamma_i i}$	Active power flow from parent node Γ_i to node i
P_{d_i}	Active load demand at node i
p_i	Aggregated active power EV and BSS injection at node i
$R_{\Gamma_i i}$	Resistance on the line between node Γ_i and i
V_i	Voltage at node i
v_i	Square of the voltage at node i
$X_{\Gamma_i i}$	Reactance on the line between node Γ_i and i

Definition of Sets

$\mathcal{E}$	Set of distribution lines
$\mathcal{L}$	Set of edges in a networked system i
$\mathcal{N}$	Set of nodes/buses.
$\mathcal{N}_i$	Set of neighboring nodes/buses of node/bus i
$\mathcal{V}$	Set of agents in a networked system i

I. INTRODUCTION

In recent times, the number of Electric Vehicles (EVs) in the distribution grid has increased in large numbers due to the attention from leading automotive industries and the government's push to reduce its greenhouse gas emissions. Consumers are also choosing EVs as their primary vehicle due to the development of charging infrastructure, upgraded battery capacity, and comparable price [1]. Due to this, EV sales in the United States have tripled between 2014 and 2018 [2]. Also, photo-voltaic (PV) solar power is becoming one of the most promising renewable energy technologies in the world which is backed by the fact that its total capacity has reached to 430GW by the end of 2018 [3]. But due to its inherent stochastic nature, PVs are usually associated with battery storage systems (BSS) which stores energy from the PVs and can inject energy on demand. Due to the penetration of these technologies, as a consequence, a high number of EV caused substantial degradation in the efficiency and reliability of the distribution power grid [4]. Also shown in [5], an uncontrolled PV with BSS can cause voltage problems which would affect the grid's

This work was supported in part by the U.S. Department of Energy under awards DEEE0006340, DE-EE0007998 and DE-EE0009028, by the U.S. National Science Foundation under grant ECCS-1308928, by the U.S. Department of Transportation under award DTRT13GUTC51.

security and even cause physical damage to equipment. As shown in [6], [7], a large number of EV charging at the same time without proper control can lead to abrupt energy peaks and an overall reduction in power quality. This scenario can also lead to an increase in power loss during transmission and a significant voltage drop in the distribution buses. Despite all these adverse effects, most researchers agree that a large number of EVs is a valuable resource that can be controlled to benefit the grid [8].

Over the years, different control schemes have been proposed in the literature. In [9], a centralized optimization scheme was presented to minimize the charging rates and facilitate voltage regulation, but it poses a scalability issue since an increase in the number of vehicles increases the number of control variables adversely. The authors in [10] proposed a centralized optimization framework to minimize the total charging cost based on time-of-use price. Although shown to have good results, however, the authors did not consider the appearance of new load peaks in low price regions causing disruption in the grid operation. Though the centralized schemes presented in [11]–[13] have simpler algorithm design, in practicality, it creates high computational complexity and requires high communication bandwidth for centralized data pooling. For these reasons, researchers in recent studies started looking into distributed architectures for controlling EVs.

In most of the distributed control strategies, third party entities called aggregators are considered which acts as a bridge between the Distribution System Operators (DSO) and the EVs [14]. The major purpose of the aggregators is to collect EV information, communicate and send input signals to the EVs based on control strategies, thus taking care of the scaling issues as the number of EVs keep increasing in the grid [15], [16]. As for the BSSs, the authors in [17], used an aggregator to coordinate a number of BSSs to provide primary frequency control services. In [18], to make the problem into a distributed one, decomposition techniques are applied in the joint optimization of optimal power flow and EV charging and is solved in a nested fashion. A primal-dual subgradient method is implemented in [19] for EV control in a residential distribution network. Although the aforementioned works provide us with a good EV charging algorithm, they somewhat fail to address the network level constraints like voltage fluctuation due to EV control in the distribution grid. In [20], a multi-agent system is presented for EV charging control. The authors investigate the bidding strategy for EV energy injection into the grid and propose energy management strategies based on it. The authors in [21] implemented a two-layer model predictive control to improve the response of BSSs for primary frequency control. Another multi-agent based control structure is proposed in [22] where the authors' design EV charging based on several study factors such as driver behavior, location of charging station, electricity price, etc. In both cases above, the authors focused on the EVs and their charging strategy but did not focus on the distribution grid and how their algorithm is affecting the grid. The work in [23] presents a chance-constrained energy management system based on ADMM where the authors tackle the stochastic randomness of the EVs and solve an EV charging scheduling optimization problem. The solution presented tackles the randomness of the EVs well but failed to show how the proposed charging solution affects the distribution grid. The authors in [24] present a distributed ADMM based multi-period problem where the DSO solved optimal power flow problems with high penetration of EV which are controlled by the aggregators. In their problem, they also ensure that grid security parameters like voltage bound and transmission line limits are maintained. A similar kind of objective of EV charging while maintaining voltage in the grid is also proposed in [25]. In this case, the authors tackled non-separable objective function with coupled power flow constraints and solved it in a decentralized way by providing a hierarchical method based on ADMM. In the above-cited works based on ADMM, iterative methods were used which are in discrete time, and thus the accuracy of the results greatly depends on the sampling time. Due to the intermittent nature of EV charging in the distribution grid, a very small sampling time is preferred to solve for the optimization dynamics in real-time otherwise the optimal solution obtained for a time step might not remain optimal anymore. The work in [4] presented a real-time solution to EV charge scheduling through a dynamic non-cooperative game approach. The authors used ADMM to decompose the centralized problem and realize the solution in real-time. The results are very interesting considering real-time application but then again, the impact of the charging scheduling on the distribution grid parameters like the voltage is neglected in the study.

Given the shortcomings of the existing research, the paper studies a real-time ADMM algorithm to be used to schedule EV and BSS charging/discharging through aggregators while maintaining the voltage profile of the grid. The contribution of this paper is two-fold: First, we present a novel continuous-domain real-time ADMM algorithm to solve networked multi-agent systems' control problems distributively. With the advent of 5G technologies and smart sensing devices, it is practically possible to obtain data from the field in one-second resolution [26] and implement a control structure in real-time. The existing literature of EV and BSS charging combined with a power flow problem is solved iteratively which takes several minutes, thus not utilizing a fair share of the data available as well as not robust to changes that are prevalent in the distribution system with distributed energy resources. Also, since all the parameters in a power grid are in the continuous domain, we can use the proposed algorithm to implement a real-time control. Secondly, we formulate an optimization problem in the distribution system with EV and BSS penetration. By using the bi-directional energy transfer capabilities of EVs using a built-in DC-AC converter, EVs and BSSs can be treated as any other distributed energy resources present in the grid [27], [28]. We set up a distributed optimization problem with power flow equations as the constraint where aggregators establish a contract with EV and BSS owners enabling them to use them as energy resources for voltage regulation while compensating the owners financially. Since the algorithm is in continuous domain and real-time, the aggregators can have a real-time update of each EV and BSS state of charge and only use

them when their state of charge is above a certain predefined threshold which is agreed through the contract. We solve the problem using our developed algorithm and show that the EV and BSS charge scheduling can be handled in real-time while keeping the distribution grid parameters within tolerable limits.

The remainder of the paper is organized as follows: In Section II, We formulate the distributed EV and BSS charging optimization problem with the power flow constraints. In section III, we develop the proposed ADMM algorithm, convert it into the continuous domain, and implement it to solve the optimization problem as a real-time control solution. Simulations were performed on a distribution system with EV penetration and the results are presented in Section IV. And, Section V contains the conclusion of our work.

II. Problem Formulation

In this section, we develop the aggregator architecture with EV and BSS and establishes a communication protocol between them. We also present the branch flow model of the distribution grid with aggregators and formulate the optimization problem.

A. Architecture of EV/BSS Aggregators

In the distribution system, we have a hierarchical communication structure. On the top is the Distribution System Operator (DSO) who is responsible for Optimal Power Flow (OPF) calculations and voltage regulation at each node of the grid. Then, on the second layer, we assume the existence of a third party entity, generally termed as "aggregator" in the literature, which can collect and dispatch the aggregate information of the EVs [24] and BSSs [29]. The EV and BSSs owners can establish a contract with a local aggregator allowing them to be utilized for grid purposes in real-time if it is between a certain State of Charge (SOC) range and in return, they will be compensated financially. More specifically, the aggregator calculates the aggregated capacity of active power based on EVs' and BSS's SOC and their operational constraint. The aggregators work in tandem with the DSO for OPF calculation and voltage regulation and work as a "middleman" between the DSO and fleet of EVs and BSSs. And finally, in the bottom layer, we have the EVs and BSS. When they are connected to the grid, either through commercial means or residential outlets, the can chose to connect with an aggregator sensor network for ancillary services and share only their SOC and power input/output, thus maintaining the privacy of the owners. The aggregators provide input signals through the same sensor network and ask the EVs or BSSs to inject power into the grid based on the OPF calculations. The coupling between an aggregator and its clients are through the sensor network, and the aggregator keeps their individual information confidential. There is no communication needed among the EVs or among the BSSs. Between the aggregators, their communication is limited to aggregated power injections. So is the communication between DSO and any of the aggregators. The communication structure between all the entities including the variables that they handle is illustrated in figure 1. In this network structure, we assume the network of DSO and the

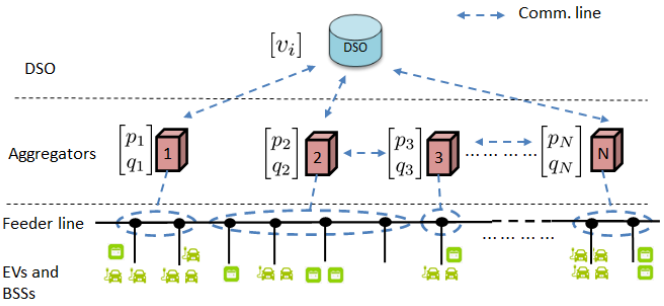

Fig. 1: The communication structure of aggregators.

aggregators are strongly connected. The DSO acts as the leader of the network and we assume it is a globally reachable node in the sense that all other nodes can be reached from the globally reachable node by following the directed branches [30]. Thus, the DSO can get all the parameters of the distribution grid through cluster of networks formed by the aggregators if it so desires, and thus, does not need to connect with all the aggregators in the topology. It should be noted that the EVs and BSSs can decide to connect to any aggregator whose sensor network is in range of them based on the compensation rates the aggregator is offering. We assume that the aggregators can communicate among themselves, thus, if there are multiple EVs or BSS under the same node connected to different aggregators, they can exchange information and can obtain the total aggregated power injection by EV and BSS at that particular node.

B. Branch Flow Model of Power Distribution Network

The branch flow model was first proposed in [31] which has better numerical stability than the branch injection model. Consider a radial distribution network by a directed graph $G = (\mathcal{N}, \mathcal{E})$ where $\mathcal{N} := \{1, \cdots, N\}$ represents the set of buses and $\mathcal{E}$ represents the set of distribution lines connecting the buses in $\mathcal{N}$. Without any loss of generality, the substation of the radial network is indexed by 1. Each node $i \in \mathcal{N} \setminus 1$ has an unique parent node Γ_i and a set of children nodes, denoted by $\mathcal{C}_i$ as shown in figure 2. We assume each directed line points towards its children, i.e., power flows from parent Γ_i to node i. We also assume all the parameters are exact and are free of uncertainty.

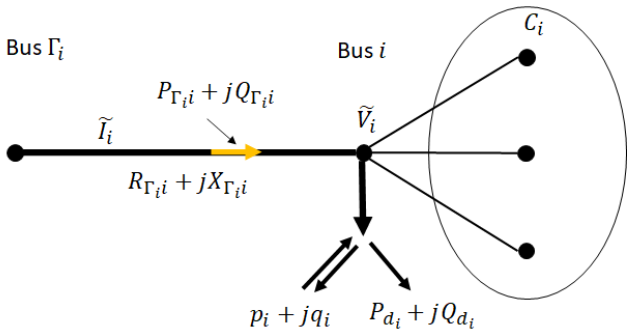

Fig. 2: A distribution network.

For each bus $i \in \mathcal{N}$, V_i is its voltage with $P_{d_i} + jQ_{d_i}$ being the load demand and $p_i + jq_i$ is the aggregated active

and reactive power injection by the aggregated EV and BSS since they are capable of producing both active and reactive power using four-quadrant charging [32]. Voltage regulation using EV and BSS reactive capacity is studied in [33] as well. For the branch $\Gamma_i \to i$, I_i is the current flowing through it with $R_{\Gamma_i i}+jX_{\Gamma_i i}$ being the impedance of the line and $P_{\Gamma_i i}+jQ_{\Gamma_i i}$ being the complex power flowing from the parent Γ_i to node i. For bus $i \in \mathcal{N} \setminus 1$, the power balance equations are given as

$$P_{\Gamma_i i} = p_i + P_{d_i} + \sum_{j \in \mathcal{C}_i} (P_{ij} + R_{ij} l_{ij}) \qquad i \in \mathcal{N} \setminus 1 \tag{1}$$

$$Q_{\Gamma_i i} = q_i + Q_{d_i} + \sum_{j \in \mathcal{C}_i} (Q_{ij} + X_{ij} l_{ij}) \qquad i \in \mathcal{N} \setminus 1 \tag{2}$$

where $l_{ij} = I_i^2$ is the square of current magnitude which is defined as

$$l_{ij} = \frac{P_{ij}^2 + Q_{ij}^2}{v_i} \tag{3}$$

where $v_i = V_i^2$ is the square of the voltage magnitude. It should be noted that the set of children for leaf nodes are null and empty. Equation (3) is a non-linear equation which can be linearized [34] around current operating point P_{ij}^o, Q_{ij}^o, v_i^o and l_{ij}^o as below:

$$\begin{aligned} l_{ij} - l_{ij}^o = & \frac{2P_{ij}^o}{v_i^o}(P_{ij} - P_{ij}^o) + \frac{2Q_{ij}^o}{v_i^o}(Q_{ij} - Q_{ij}^o) \\ & - \frac{(P_{ij}^o)^2 + (Q_{ij}^o)^2}{(v_i^o)^2}(v_i - v_i^o) \end{aligned} \tag{4}$$

For the substation bus, equations (1) and (2) takes the following form

$$0 = p_1 + P_{d_1} + \sum_{j \in \mathcal{C}_1} (P_{1j} + R_{1j} l_{1j}) \tag{5}$$

$$0 = q_1 + Q_{d_1} + \sum_{j \in \mathcal{C}_1} (Q_{1j} + X_{1j} l_{1j}) \tag{6}$$

The power flow on all lines $(i,j) \in \mathcal{E}$ are expressed as

$$v_i - v_j = 2(R_{ij}P_{ij} + X_{ij}Q_{ij}) + (R_{ij}^2 + X_{ij}^2) l_{ij} \tag{7}$$

The voltage magnitude limits are given by

$$v_i^{min} \le v_i \le v_i^{max} \qquad \forall i \in \mathcal{N} \tag{8}$$

From the study done by the authors in [35], the distribution line maximum current flow constraint should take into account the current that flows in the charging susceptance of the line. For line $(i,j) \in \mathcal{E}$, the thermal limit constraint is given as

$$l_{ij} + \frac{1}{4} B_{ij}^2 v_i + B_{ij} Q_{ij} \le l_{ij}^{max} \tag{9}$$

$$l_{ij} + \frac{1}{4} B_{ij}^2 v_j + B_{ij}(X_{ij} l_{ij} - Q_{ij}) \le l_{ij}^{max} \tag{10}$$

Let us define set of feasible points which satisfy the inequality (8) as follows:

$$\mathcal{S}_v = \{v_i : (8) \qquad \forall i \in \mathcal{N}\}, \tag{11}$$

and the inequalities (9) and (10) as follows:

$$\mathcal{S}_l = \{l_{ij} : (9) - (10) \qquad \forall j \in \mathcal{N}_i, i \in \mathcal{N}\}. \tag{12}$$

C. Objective Functions

The EV and BSS owners sign a contract with the aggregators to maximize their monetary gain by providing voltage regulation as well as minimize the cost incurred due to charging. Let us define a utility function $U_i(p_i, q_i), i \in \mathcal{N}$ which is concave in nature and expresses the monetary satisfaction of all the EV and BSS connected at the ith bus. Thus, we can define the owners welfare function $W_i(p_i, q_i)$ at each bus as follows:

$$W_i(p_i, q_i) = \psi p_i - U_i(p_i, q_i) \qquad i \in \mathcal{N} \tag{13}$$

where ψ is the price of electricity. The meaning of the welfare function $W_i(p_i, q_i)$ simple. The EV and BSS incur expense ψp_i by charging their batteries from the grid and PVs, but by providing services like voltage regulation, they can earn revenue defined by the concave function $U_i(p_i, q_i)$. The overall welfare function $\sum_{i \in \mathcal{N}} W_i(p_i, q_i)$ is convex in nature since its an addition of a straight line and a negative concave function. It should be noted that the welfare function is a function of aggregated power by the aggregators at each node. The aggregators use only those EV and BSS whose SOCs are inside a predefined range. The aggregator then compensates the owners based on the contract agreement. Since this work only deals with the DSO and aggregator layer, it is beyond the scope of this paper to define the aggregator-EV or aggregator-BSS relationship and how the aggregator compensates them. This issue would be addressed in our future work. For the grid, the DSO and the aggregators want to use the EV and BSS to maintain the voltage at each node close to 1p.u. which can be expressed by the following penalty function which is quadratic and is thus convex:

$$H_i(v_i) = (1 - v_i)^2 \qquad i \in \mathcal{N} \tag{14}$$

Therefore, we can define the optimization problem for the whole network as follows:

$$J(p, q, v) = \sum_{i \in \mathcal{N}} J_i(p_i, q_i, v_i) \tag{15}$$

$$\begin{aligned} \text{where} \quad & J_i(p_i, q_i, v_i) = k_i W_i(p_i, q_i) + (1 - k_i) H_i(v_i) \\ \text{s.t.} \quad & v_i \in \mathcal{S}_v, l_{ij} \in \mathcal{S}_l \\ & (1), (2), (4) - (7) \end{aligned} \tag{16}$$

where $0 < k_i < 1$ is the weight on each objective function. The aggregators sum up all the EV and BSS power potential at each node and try to minimize the welfare function $\sum_{i \in \mathcal{N}} W_i(p_i, q_i)$ for their customers. The DSO works with the aggregators to obtain EV and BSS injection information at each node and wants to maintain a unity voltage profile $\sum_{i \in \mathcal{N}} H_i(v_i)$ in the grid while solving the power flow in the process. In the next section, we will develop a continuous-domain distributed ADMM algorithm to solve problem (15) in real-time.

III. Continuous-Domain Distributed ADMM Algorithm

In this section, we develop the continuous-domain real-time ADMM algorithm which can be implemented to a broad class

of networked multi-agent distributed optimization and control problems. Then, we show our optimization problem, which is a special case, can be solved distributively using the developed ADMM method in the continuous domain.

A. Network of Agents

Let us consider a networked multi-agent system which is characterized by a bidirectional graph $\mathcal{G} = (\mathcal{V}, \mathcal{L})$ where $\mathcal{V} = \{1, 2, \cdots, N\}$ is the number of agents and $\mathcal{L}$ represents the set of edges between them. Also, let node 1 be the virtual leader of the network which means, through the communication network, node 1 can obtain the information of all the nodes in the network if necessary. We can define the network interconnection with the following binary matrix [30]:

$$S = \begin{bmatrix} 1 & 1 & \cdots & 1 \\ 1 & 1 & \cdots & s_{2N} \\ \vdots & \vdots & \vdots & \vdots \\ 1 & s_{N2} & \cdots & 1 \end{bmatrix}, \tag{17}$$

where $s_{ij} = 1$ if and only if $(i \leftrightarrow j) \in \mathcal{L}$, and $s_{ij} = 0$ if otherwise. The matrix S has 1 in the diagonal as every agent knows its own information. We have the following assumption which ensures the connectivity of the network.

Assumption 1: *The matrix S is irreducible, i.e., the communication graph is strongly connected.*

Using the communication matrix S, let us also define a gain matrix D whose values are calculated according to the following equation:

$$D = [d_{ij}] \in \mathbb{R}^{N \times N}, \quad d_{ij} = \frac{s_{ij}\beta_{ij}}{\sum_{l=1}^{N} s_{il}\beta_{il}}, \tag{18}$$

where $\beta_{ij} > 0$ are piecewise-constant scalar gains. The matrix D is a non-negative, row stochastic and diagonally positive matrix.

B. Distributed Real-Time Continuous Domain ADMM

Let us consider the following optimization problem

$$\min \quad \sum_{i \in \mathcal{V}} f_i(x_i) \tag{19a}$$

$$\text{s.t.} \quad \sum_{j \in \mathcal{V}_i} A_{ij} x_j = 0 \quad \text{for} \quad i \in \mathcal{V}, \tag{19b}$$

For agent i, $\mathcal{V}_i$ denotes the set of its neighboring agents including itself, $x_i \in \mathbb{R}^n$ is its state vector, $f_i(x_i)$ is its objective function, and A_{ij} are matrices of appropriate dimensions which represents the interconnection between the agents. The following assumption is made on the individual objective functions.

Assumption 2: *Functions f_i, $i \in \mathcal{V}$, are convex and differentiable, and their gradients denoted by $\nabla_{x_i} f_i(x_i)$ are Lipschitz continuous. The set of optimal solutions to* (19) *is not empty, and the corresponding minimum of* (19a) *is finite.*

The goal is to develop a distributed algorithm so that each agent can solve problem (19a) while satisfying the linear constraint (19b) by exchanging relevant information with its neighboring agents. The problem (19) can be solved using ADMM by reformulating it using a secondary variable z_{ji}, which represents the observation of the variables of agent j at agent i. We can then reformulate (19) as follows [36]:

$$\min \quad \sum_{i \in \mathcal{V}} f_i(x_i) \tag{20a}$$

$$\text{s.t.} \quad \sum_{j \in \mathcal{V}_i} A_{ij} z_{ji} = 0 \quad \text{for} \quad i \in \mathcal{V} \tag{20b}$$

$$x_i = z_{ij} \qquad j \in \mathcal{V}_i, \;\; i \in \mathcal{V} \tag{20c}$$

where x and z represents the two set of variables in standard ADMM [37]. In the consensus constraint (20c), the observations z_{ij} are forced to equal to the state variable x_i, thus the optimal solution to the problem (20) is also optimal to the original problem (19). It should be noted that in problem (20), (20b) involves only z but (20c) contains both x and z. Hence, we form the so called "augmented Lagrangian" as follows:

$$L(x, z, \lambda) = \sum_{i \in \mathcal{V}} L_i(x_i, z_{ij}, \lambda_{ij}), \tag{21}$$

$$L_i = f_i(x_i) + \sum_{j \in \mathcal{V}_i} \left[d_{ij} \lambda_{ij}^T (x_i - z_{ij}) + \frac{d_{ij}}{2} ||x_i - z_{ij}||^2 \right]$$

where λ_{ij} is the dual variable. In the proposed multi-agent ADMM algorithm, the usual constant penalty term is replaced with d_{ij} from D matrix defined in (18). This enables the penalty term to conform with the actual physical interconnection of the agents [36]. Because of this reason, the Lagrange multiplier λ_{ij} is also scaled by it. The following theorem provides the continuous-domain solution to the augmented Lagrangian (21) whose proof is provided in the Appendix.

Theorem 1: *The augmented Lagrangian* (21) *can be solved in the continuous domain using the following dynamics:*

$$\dot{x}_i = -\alpha_i' \left[\nabla_{x_i} f_i(x_i) + \sum_{j \in \mathcal{V}_i} d_{ij} \left[\lambda_{ij} + (x_i - z_{ij}^-) \right] \right] \tag{22a}$$

$$\dot{z}_{ji} = \alpha_i' [d_{ji} \lambda_{ji} + d_{ji}(x_j - z_{ji}) - A_{ij}^T \mu_i] \tag{22b}$$

$$\dot{\mu}_i = \sum_{j \in \mathcal{V}_i} A_{ij} z_{ji} \tag{22c}$$

$$\dot{\lambda}_{ji} = d_{ji}(x_j - z_{ji}), \tag{22d}$$

where $z_{ij}^-(t) \triangleq z_{ij}(t - \Delta)$ for some $\Delta > 0$ is a delayed version of z_{ij}.

The above set of dynamic equation (22) provides us with the optimal solution to the problem (20). The convergence results of theorem 1 are summarized in lemma 1 and the proof is provided in the Appendix.

Lemma 1: *Under assumptions 1 and 2, the distributed ADMM algorithm* (22) *is convergent to an optimal solution.*

C. Real-Time ADMM Solution to EV/BSS Management

In this subsection, we show that the optimization problem (15) can be solved in a distributed manner using the above method. The aggregators at each bus and DSO can be considered as agents in the distribution power network. They communicate relevant information among them for OPF calculation and maintaining voltage regulation. The DSO is the global leader as node 1 in setting power dispatch signal, each of the aggregators is a local agent which interacts with its cluster of EVs and BSS that are grouped based on their locations, and neighboring aggregators may communicate with each other. Nonetheless, the DSO does not have global information, as its communication with an aggregator is limited to the aggregated dispatch signal for that cluster. Similarly, the communication among aggregators only contain the information about aggregated injections. Thus the communication topology between the aggregators and DSO can be represented by the communication matrix (17). Agent i has the information of its own voltage v_i, the aggregated active and reactive power injection p_i, q_i. It also has the information of the amount of active power, reactive power and current that is coming from its parent node. Thus, at agent i, we can define the state variables as $x_i = [v_i, p_i, q_i, P_{\Gamma_i i}, Q_{\Gamma_i i}, l_{\Gamma_i i}]^T$. To solve the problem using continuous-domain ADMM, we introduce an observation vector z_{ji}, which represents the variables of node j observed at node i as $z_{ji} = [v_j^i, p_j^i, q_j^i, P_{\Gamma_j j}^i, Q_{\Gamma_j j}^i, l_{\Gamma_j j}^i]^T$ [36]. With these vector definitions, we can redefine the problem (15) according to our developed distributed ADMM problem (20) as follows

$$\min_{x_i} \quad \sum_{i\in\mathcal{N}} J_i(x_i) + \mathcal{I}_{v_i} + \mathcal{I}_{l_{ij}} \tag{23a}$$

$$\text{s.t.} \quad \sum_{j\in\mathcal{N}_i} A_{ij} z_{ji} + m_{ji} = 0 \qquad \forall i \in \mathcal{N} \tag{23b}$$

$$x_i = z_{ij} \qquad \forall i \in \mathcal{N} \tag{23c}$$

$$v_i \in \mathcal{S}_v, l_{ij} \in \mathcal{S}_l \tag{23d}$$

where $\mathcal{N}_i \triangleq \{\Gamma_i\} \cup \{i\} \cup \mathcal{C}_i$. $\mathcal{I}_{v_i}$ anr $\mathcal{I}_{l_{ij}}$ are indicator functions defined as :

$$\mathcal{I}_{v_i} = \begin{cases} 0, & v_i \in \mathcal{S}_{v_i} \\ \infty & \text{otherwise.} \end{cases} \tag{24}$$

$$\mathcal{I}_{l_{ij}} = \begin{cases} 0, & l_{ij} \in \mathcal{S}_{l_{ij}} \\ \infty & \text{otherwise.} \end{cases} \tag{25}$$

Equation (23b) is based on equations (1)-(7). Thus, we can define the matrix A_{ij}, based on which agent j represents, as follows

$$A_{ii} = \begin{bmatrix} 0 & 1 & 0 & -1 & 0 & 0 \\ 0 & 0 & 1 & 0 & -1 & 0 \\ 1 & 2R_{\Gamma_i i} & 2X_{\Gamma_i i} & 0 & 0 & (R_{\Gamma_i i}^2 + X_{\Gamma_i i}^2) \\ 0 & 0 & 0 & \frac{2P_{\Gamma_i i}^o}{v_{\Gamma_i}^o} & \frac{2Q_{\Gamma_i i}^o}{v_{\Gamma_i}^o} & -1 \end{bmatrix}$$

$$A_{ij} = \begin{bmatrix} 0 & 0 & 0 & 1 & 0 & R_{ij} \\ 0 & 0 & 0 & 0 & 1 & X_{ij} \\ 0 & 0 & 0 & 0 & 0 & 0 \\ 0 & 0 & 0 & 0 & 0 & 0 \end{bmatrix}, \quad j \in \mathcal{C}_i,$$

$$A_{ij} = \begin{bmatrix} 0 & 0 & 0 & 0 & 0 \\ 0 & 0 & 0 & 0 & 0 \\ -1 & 0 & 0 & 0 & 0 \\ -\frac{(P_{ij}^o)^2 + (Q_{ij}^o)^2}{(v_{\Gamma_i}^o)^2} & 0 & 0 & 0 & 0 \end{bmatrix}, \quad j = \Gamma_i, \tag{26}$$

and a vector of constants

$$m_{ii} = \begin{bmatrix} P_{d_i} \\ Q_{d_i} \\ 0 \\ 0 \end{bmatrix}$$

$$m_{ij} = \begin{bmatrix} R_{ji} l_{ji} \\ X_{ji} l_{ji} \\ 0 \\ 0 \end{bmatrix} \quad j \in \mathcal{C}_i$$

$$m_{ii} = \begin{bmatrix} 0 \\ 0 \\ (R_{ji}^2 + X_{ji}^2) l_{ji} \\ -\frac{2(P_{ji}^o)^2 v_j^o + 2(Q_{ji}^o)^2 v_j^o + (P_{ji}^o)^2 - (Q_{ji}^o)^2}{(v_j^o)^2} - l_{ji}^o \end{bmatrix} \quad j \in \Gamma_i \tag{27}$$

For our work, we considered a balanced distribution system. For an unbalanced system, we can apply the Fortescue transformation for distribution grid [38] and update the entries of A_{ij} matrix accordingly. Following the procedure in Section III-B, we form the augmented Lagrangian using dual vector $\lambda_{ij} = [\lambda_{ij}(1), \lambda_{ij}(2), \cdots, \lambda_{ij}(6)]^T$ and using theorem 1, obtain the following continuous-domain dynamics for agent i:

x_i update dynamics for each variable:

$$\dot{v}_i = -\alpha_i^{'}\left[\nabla_{v_i} J_i(x_i) + \sum_{j\in\mathcal{N}_i} d_{ij}\Big[\lambda_{ij}(1) + (v_i - v_i^{j-})\Big]\right]$$

$$\dot{p}_i = -\alpha_i^{'}\left[\nabla_{p_i} J_i(x_i) + \sum_{j\in\mathcal{N}_i} d_{ij}\Big[\lambda_{ij}(2) + (p_i - p_i^{j-})\Big]\right]$$

$$\dot{q}_i = -\alpha_i^{'}\left[\nabla_{q_i} J_i(x_i) + \sum_{j\in\mathcal{N}_i} d_{ij}\Big[\lambda_{ij}(3) + (q_i - q_i^{j-})\Big]\right]$$

$$\dot{P}_{\Gamma_i i} = -\alpha_i^{'}\left[\nabla_{P_{\Gamma_i i}} J_i(x_i) + \sum_{j\in\mathcal{N}_i} d_{ij}\Big[\lambda_{ij}(4) + (P_{\Gamma_i i} - P_{\Gamma_i i}^{j-})\Big]\right]$$

$$\dot{Q}_{\Gamma_i i} = -\alpha_i^{'}\left[\nabla_{Q_{\Gamma_i i}} J_i(x_i) + \sum_{j\in\mathcal{N}_i} d_{ij}\Big[\lambda_{ij}(5) + (Q_{\Gamma_i i} - Q_{\Gamma_i i}^{j-})\Big]\right]$$

$$\dot{l}_{\Gamma_i i} = -\alpha_i\left[\nabla_{l_{\Gamma_i i}} J_i(x_i) + \sum_{j\in\mathcal{N}_i} d_{ij}\Big[\lambda_{ij}(6) + (l_{\Gamma_i i} - l_{\Gamma_i i}^{j-})\Big]\right]$$

The auxiliary primal variable z_{ji} update dynamics is given as:

$$\begin{bmatrix} \dot{v}_j^i \\ \dot{p}_j^i \\ \dot{q}_j^i \\ \dot{P}_{\Gamma_j j}^i \\ \dot{Q}_{\Gamma_j j}^i \\ \dot{l}_{\Gamma_j j}^i \end{bmatrix} = \alpha_i^{'} d_{ji} \begin{bmatrix} \lambda_{ji}(1) \\ \lambda_{ji}(2) \\ \lambda_{ji}(3) \\ \lambda_{ji}(4) \\ \lambda_{ji}(5) \\ \lambda_{ji}(6) \end{bmatrix} + d_{ji} \begin{bmatrix} v_j - v_j^i \\ p_j - p_j^i \\ q_j - q_j^i \\ P_{\Gamma_j j} - P_{\Gamma_j j}^i \\ Q_{\Gamma_j j} - Q_{\Gamma_j j}^i \\ l_{\Gamma_j j} - l_{\Gamma_j j}^i \end{bmatrix} - A_{ij}^T \begin{bmatrix} \mu_i(1) \\ \mu_i(2) \\ \mu_i(3) \\ \mu_i(4) \\ \mu_i(5) \\ \mu_i(6) \end{bmatrix}$$

The dual updates are given as follows:

$$\begin{bmatrix} \dot{\mu}_i(1) \\ \dot{\mu}_i(2) \\ \dot{\mu}_i(3) \\ \dot{\mu}_i(4) \\ \dot{\mu}_i(5) \\ \dot{\mu}_i(6) \end{bmatrix} = \sum_{j\in\mathcal{N}_i} A_{ij} \begin{bmatrix} v_j^i \\ p_j^i \\ q_j^i \\ P_{\Gamma_j j}^i \\ Q_{\Gamma_j j}^i \\ l_{\Gamma_j j}^i \end{bmatrix}$$

$$\begin{bmatrix} \dot{\lambda}_{ji}(1) \\ \dot{\lambda}_{ji}(2) \\ \dot{\lambda}_{ji}(3) \\ \dot{\lambda}_{ji}(4) \\ \dot{\lambda}_{ji}(5) \\ \dot{\lambda}_{ji}(5) \end{bmatrix} = d_{ji} \begin{bmatrix} v_j - v_j^i \\ p_j - p_j^i \\ q_j - q_j^i \\ P_{\Gamma_j j} - P_{\Gamma_j j}^i \\ Q_{\Gamma_j j} - Q_{\Gamma_j j}^i \\ l_{\Gamma_j j} - l_{\Gamma_j j}^i \end{bmatrix}$$

where A_{ij} are defined in (26).

IV. Simulation results

In this section, the proposed distributed continuous-domain real-time ADMM algorithm is implemented on the IEEE 123 bus distribution system with EV penetration. First, we simulated a base case with no EV penetration and control to set up a reference point for the simulation. Then we included EVs into the system and implemented our proposed algorithm for EV welfare and voltage optimization with power flow equations as constraints.

First, we set up the IEEE 123 bus distribution system in OpenDSS and ran the base case without any control whose voltage profile is shown in figure 3. Then we introduced 200 EVs of different capacities and types into the grid which can be aggregated among 40 buses. Table I summarises the different types of input power injection range for EVs and table II shows the types of EVs used in the study and their corresponding battery capacity [39]. Based on the data from the table, we ran models of EV with randomized initial SOC over a certain period of time to come with a range of SOC, and only those EVs were used whose SOC were bounded between 80 to 100 percent. In the simulation, the welfare function is defined as a quadratic function: $W_i(p_i, q_i) = a_p p_i^2$ with the value of coefficients taken from the literature [40] and the price of electricity was fixed at an average of 15 cents per kWh. Although the algorithm is capable of handling it, we assumed the EVs only inject active power in this scenario and the total aggregated reactive power injection is 0. To measure the convergence to steady-state, we defined the primal residual as $\max_i \sum_{j\in\mathcal{N}_i} |x_i - z_{ij}^-|$, and the dual residual as $\max_i \sum_{j\in\mathcal{N}_i} |z_{ij} - z_{ij}^-|$ [36], [37]. In the implementation of the algorithm, we chose $\alpha_i^{'}$ to be the same for each node with a value of 0.01 and weight k_i is chosen to be 0.2. In the simulation scenarios, we kept the generation from the sub-station at a fixed point equal to the minimum loading conditions. We introduced 100 intermittent photo-voltaic (PV) resources spread across the distribution grid with a random generation profile. We also created a random loading profile where the spot loads at each node vary over time. We introduced our algorithm to all the 40 aggregators to compensate for the intermittent renewable generation and random loading with the objective of keeping the voltage profile within tolerable range as well as maximizing their utilization function. In our simulation, we assumed that there is always enough EVs with acceptable SOC range to compensate for voltage regulation. The simulation was run for 5 hours to observe the impact on the node voltages.

TABLE I: EV charging categories

Charging method	Voltage	Max. current	Input power
AC level 1	120 V	12 A	1.4 kW
AC level 2	208 - 240 V	32 A	7.2-19.2 kW
DC charging	400 - 1000 V	300 A	50-150 kW

From the base case, we identified three nodes, namely node 111,113, and 114, which have the three lowest nodal voltage without control in the circuit. Figure 4 shows the evolution of the voltages in those three nodes over the five hours where control was applied. Figure 5 shows the total

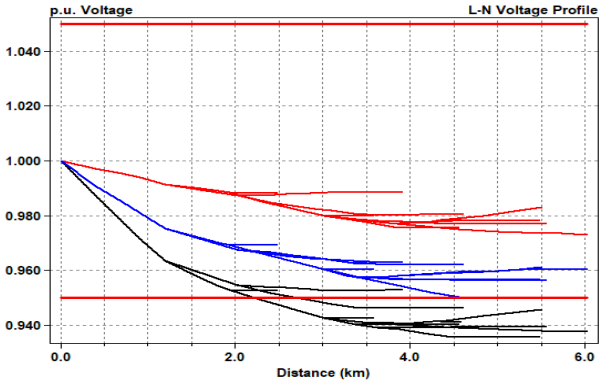

Fig. 3: Voltage profile of the base case

TABLE II: EV Types

Brand name	Battery capacity
Nissan Leaf	40-62 kWh
Toyota RAV4-EV	41.8 kWh
BMW i3	42.2 kWh
Tesla model 3	75 kWh
Tesla model S	100 kWh
Tesla model X	100 kWh

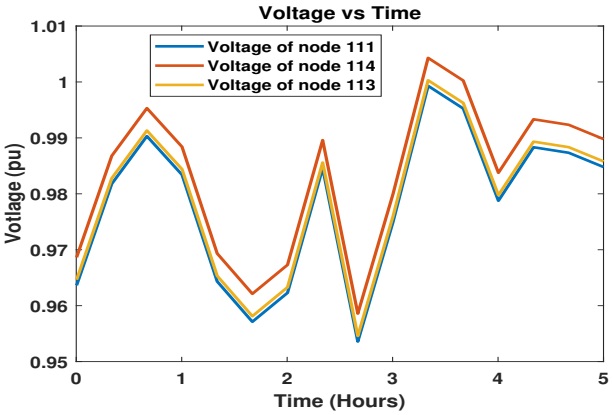

Fig. 4: Voltages at node 111,113 and 114

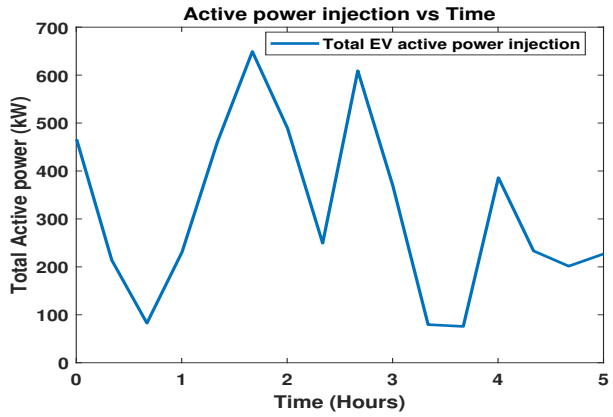

Fig. 5: Total active power injection by EVs into the grid

injection of active power into the grid by the EVs. It can be seen from both the figure that whenever there is a rise in voltage (between time period 0-1 hour and time period 3-4 hour) due to more generation from the intermittent renewable resources or lower loading condition, the total EV active power injection decreases which means they are charging. The opposite happens whenever there is a loss in voltage due to higher loading conditions or loss of renewable resources, the EVs start discharging which maintains the voltage above the lower limit of 0.95 pu. In this way the algorithm makes sure the EV injection follows the voltage profile. Figure 6 shows the steady-state voltage at each node of the test circuit.

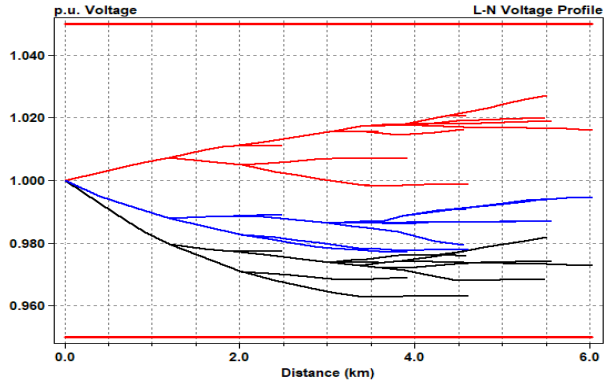

Fig. 6: Steady state voltage output after using the algorithm

V. Conclusion

In this paper, a novel continuous-domain real-time distributed multi-agent ADMM algorithm is developed for real-time applications. A distribution system was modeled where EV and BSS owners sign contracts with aggregators to allow them to be used for ancillary services like voltage regulation in exchange for monetary gain. A convex optimization problem with power flow equations as constraints were set up where each aggregator tries to minimize the EV and BSS charging cost while contributing to ancillary services while DSO would maintain the voltage close to unity and solve the power flow. In the setup, we only consider DSO and aggregators as the acting agents in the grid and assume the aggregators can send signals to EVs and BSSs to alter their power injection in the grid. We assume the SOC of EVs and BSSs are within a predefined agreed-upon range and there is enough EV and BSS reserve for ancillary services. In our future work, we would consider EV and BSS optimization with aggregator connection and also tackle SOC evolution which is dynamic in nature. The developed problem with DSO and aggregators was cast into a distributed ADMM framework and is solved using the proposed continuous-domain real-time algorithm by communicating relevant information among them. In contrast to usual discrete-time iterative solution techniques where the accuracy and optimality of the solution depend on the sampling and convergence time, the proposed continuous-domain algorithm can solve the optimization and control problems in real-time. Numerical simulations were carried out on IEEE 123 bus distribution grid to show the effectiveness of the proposed algorithm.

REFERENCES

[1] L. Cai, J. Pan, L. Zhao, and X. Shen, "Networked electric vehicles for green intelligent transportation," *IEEE Communications Standards Magazine*, vol. 1, no. 2, pp. 77–83, 2017.

[2] I. Wagner, *The U.S. Electric Vehicle Industry - Statistics and Facts*, 2020 (April 30). [Online]. Available: https://www.statista.com/topics/4421/the-us-electric-vehicle-industry/

[3] Y. Zhang, K. Meng, F. Luo, H. Yang, J. Zhu, and Z. Y. Dong, "Multi-agent-based voltage regulation scheme for high photovoltaic penetrated active distribution networks using battery energy storage systems," *IEEE Access*, vol. 8, pp. 7323–7333, 2019.

[4] L. Chen, T. Yu, Y. Chen, W. Guan, Y. Shi, and Z. Pan, "Real-time optimal scheduling of large-scale electric vehicles: A dynamic non-cooperative game approach," *IEEE Access*, vol. 8, pp. 133 633–133 644, 2020.

[5] J. Tuominen, S. Repo, and A. Kulmala, "Comparison of the low voltage distribution network voltage control schemes," in *IEEE PES Innovative Smart Grid Technologies, Europe*. IEEE, 2014, pp. 1–6.

[6] M. Li, J. Gao, N. Chen, L. Zhao, and X. Shen, "Decentralized pev power allocation with power distribution and transportation constraints," *IEEE Journal on Selected Areas in Communications*, vol. 38, no. 1, pp. 229–243, 2019.

[7] H. Liang, Y. Liu, F. Li, and Y. Shen, "Dynamic economic/emission dispatch including pevs for peak shaving and valley filling," *IEEE Transactions on Industrial Electronics*, vol. 66, no. 4, pp. 2880–2890, 2018.

[8] B. Khaki, C. Chu, and R. Gadh, "A hierarchical admm based framework for ev charging scheduling," in *2018 IEEE/PES Transmission and Distribution Conference and Exposition (T&D)*. IEEE, 2018, pp. 1–9.

[9] P. Richardson, D. Flynn, and A. Keane, "Optimal charging of electric vehicles in low-voltage distribution systems," *IEEE Transactions on Power Systems*, vol. 27, no. 1, pp. 268–279, 2011.

[10] Y. Cao, S. Tang, C. Li, P. Zhang, Y. Tan, Z. Zhang, and J. Li, "An optimized EV charging model considering tou price and soc curve," *IEEE Transactions on Smart Grid*, vol. 3, no. 1, pp. 388–393, 2011.

[11] K. Clement-Nyns, E. Haesen, and J. Driesen, "The impact of charging plug-in hybrid electric vehicles on a residential distribution grid," *IEEE Transactions on power systems*, vol. 25, no. 1, pp. 371–380, 2009.

[12] S. Deilami, A. S. Masoum, P. S. Moses, and M. A. Masoum, "Real-time coordination of plug-in electric vehicle charging in smart grids to minimize power losses and improve voltage profile," *IEEE Transactions on Smart Grid*, vol. 2, no. 3, pp. 456–467, 2011.

[13] S. Shao, M. Pipattanasomporn, and S. Rahman, "Challenges of PHEV penetration to the residential distribution network," in *2009 IEEE Power & Energy Society General Meeting*. IEEE, 2009, pp. 1–8.

[14] A. Asrari, M. Ansari, J. Khazaei, and P. Fajri, "A market framework for decentralized congestion management in smart distribution grids considering collaboration among electric vehicle aggregators," *IEEE Transactions on Smart Grid*, 2019.

[15] Z. Pan, T. Yu, J. Li, K. Qu, L. Chen, B. Yang, and W. Guo, "Stochastic transactive control for electric vehicle aggregators coordination: A decentralized approximate dynamic programming approach," *IEEE Transactions on Smart Grid*, 2020.

[16] S. Gao and H. Jia, "Integrated configuration and optimization of electric vehicle aggregators for charging facilities in power networks with renewables," *IEEE Access*, vol. 7, pp. 84 690–84 700, 2019.

[17] D. Zhu and Y.-J. A. Zhang, "Optimal coordinated control of multiple battery energy storage systems for primary frequency regulation," *IEEE Transactions on Power Systems*, vol. 34, no. 1, pp. 555–565, 2018.

[18] N. Chen, C. W. Tan, and T. Q. Quek, "Electric vehicle charging in smart grid: Optimality and valley-filling algorithms," *IEEE Journal of Selected Topics in Signal Processing*, vol. 8, no. 6, pp. 1073–1083, 2014.

[19] M. Liu, P. K. Phanivong, Y. Shi, and D. S. Callaway, "Decentralized charging control of electric vehicles in residential distribution networks," *IEEE Transactions on Control Systems Technology*, vol. 27, no. 1, pp. 266–281, 2017.

[20] H. K. Nunna, S. Battula, S. Doolla, and D. Srinivasan, "Energy management in smart distribution systems with vehicle-to-grid integrated microgrids," *IEEE Transactions on Smart Grid*, vol. 9, no. 5, pp. 4004–4016, 2018.

[21] A. Oshnoei, M. Kheradmandi, and S. Muyeen, "Robust control scheme for distributed battery energy storage systems in load frequency control," *IEEE Transactions on Power Systems*, 2020.

[22] K. Chaudhari, N. K. Kandasamy, A. Krishnan, A. Ukil, and H. B. Gooi, "Agent-based aggregated behavior modeling for electric vehicle charging load," *IEEE Transactions on Industrial Informatics*, vol. 15, no. 2, pp. 856–868, 2018.

[23] B. Wang, P. Dehghanian, and D. Zhao, "Chance-constrained energy management system for power grids with high proliferation of renewables and electric vehicles," *IEEE Transactions on Smart Grid*, vol. 11, no. 3, pp. 2324–2336, 2019.

[24] H. Fan, C. Duan, C.-K. Zhang, L. Jiang, C. Mao, and D. Wang, "Admm-based multiperiod optimal power flow considering plug-in electric vehicles charging," *IEEE Transactions on Power Systems*, vol. 33, no. 4, pp. 3886–3897, 2017.

[25] X. Zhou, S. Zou, P. Wang, and Z. Ma, "Voltage regulation in constrained distribution networks by coordinating electric vehicle charging based on hierarchical admm," *IET Generation, Transmission & Distribution*, vol. 14, no. 17, pp. 3444–3457, 2020.

[26] M. Sengupta and A. Andreas, "Oahu solar measurement grid (1-year archive): 1-second solar irradiance; oahu, hawaii (data)," National Renewable Energy Lab.(NREL), Golden, CO (United States), Tech. Rep., 2010.

[27] K. Kaur, N. Kumar, and M. Singh, "Coordinated power control of electric vehicles for grid frequency support: Milp-based hierarchical control design," *IEEE Transactions on Smart Grid*, vol. 10, no. 3, pp. 3364–3373, 2018.

[28] H. Liu, Y. Zhang, S. Ge, C. Gu, and F. Li, "Day-ahead scheduling for an electric vehicle pv-based battery swapping station considering the dual uncertainties," *IEEE Access*, vol. 7, pp. 115 625–115 636, 2019.

[29] M. Dolatabadi and P. Siano, "A scalable privacy preserving distributed parallel optimization for a large-scale aggregation of prosumers with residential pv-battery systems," *IEEE Access*, vol. 8, pp. 210 950–210 960, 2020.

[30] Z. Qu, *Cooperative Control of Dynamical Systems*. Springer, 2009.

[31] M. E. Baran and F. F. Wu, "Optimal capacitor placement on radial distribution systems," *IEEE Transactions on power Delivery*, vol. 4, no. 1, pp. 725–734, 1989.

[32] N. Mehboob, M. Restrepo, C. A. Canizares, C. Rosenberg, and M. Kazerani, "Smart operation of electric vehicles with four-quadrant chargers considering uncertainties," *IEEE Transactions on Smart Grid*, vol. 10, no. 3, pp. 2999–3009, 2018.

[33] H. V. Haghi and Z. Qu, "A kernel-based predictive model of EV capacity for distributed voltage control and demand response," *IEEE Transactions on Smart Grid*, vol. 9, no. 4, pp. 3180–3190, 2016.

[34] C. Ai, G. Zhou, W. Gao, J. Guo, G. Jie, Z. Han, and X. Kong, "Research on quasi-synchronous grid-connected control of hydraulic wind turbine," *IEEE Access*, vol. 8, pp. 126 092–126 108, 2020.

[35] M. Nick, R. Cherkaoui, J.-Y. Le Boudec, and M. Paolone, "An exact convex formulation of the optimal power flow in radial distribution networks including transverse components," *IEEE Transactions on Automatic Control*, vol. 63, no. 3, pp. 682–697, 2017.

[36] T. Rahman, Z. Qu, and T. Namerikawa, "Improving rate of convergence via gain adaptation in multi-agent distributed admm framework," *IEEE Access*, vol. 8, pp. 80 480–80 489, 2020.

[37] S. Boyd, N. Parikh, E. Chu, B. Peleato, J. Eckstein *et al.*, "Distributed optimization and statistical learning via the Alternating Direction Method of Multipliers," *Foundations and Trends in Machine learning*, vol. 3, pp. 1–122, 2011.

[38] I. Dzafic, T. Donlagic, and S. Henselmeyer, "Fortescue transformations for three-phase power flow analysis in distribution networks," in *2012 IEEE Power and Energy Society General Meeting*. IEEE, 2012, pp. 1–7.

[39] H. Wang, D. Zhao, Q. Meng, G. P. Ong, and D.-H. Lee, "A four-step method for electric-vehicle charging facility deployment in a dense city: An empirical study in singapore," *Transportation Research Part A: Policy and Practice*, vol. 119, pp. 224–237, 2019.

[40] Y. Okawa, T. Namerikawa, and Z. Qu, "Passivity-based stability analysis of dynamic electricity pricing with power flow," in *2017 IEEE 56th Annual Conference on Decision and Control (CDC)*. IEEE, 2017, pp. 813–818.

[41] A. Makhdoumi and A. Ozdaglar, "Convergence rate of distributed ADMM over networks," *IEEE Transactions on Automatic Control*, vol. 62, no. 10, pp. 5082–5095, 2017.

[42] S. Boyd and L. Vandenberghe, *Convex Optimization*. Cambridge University Press, 2004.

APPENDIX

A. Proof of Theorem 1

ADMM consists of first the x-minimization and then z-minimization, followed by the updates of the dual variables [37]. Following from the augmented Lagrangian (21), The algorithm is as follows:

1) x_i is updated according to

$$x_i^{k+1} := \underset{x_i \in \mathbb{R}^n}{\arg\min}\, L_D(x, z^k, \lambda^k, \mu^k), \tag{28a}$$

2) For $j \in \mathcal{N}_i$, z_{ji} is solved as

$$z_{ji}^{k+1} := \underset{z_{ji} \in \mathbb{R}^n}{\arg\min}\; L_D(x^{k+1}, z, \lambda^k, \mu^k) \quad \text{s.t.} \quad \sum_{j \in \mathcal{V}_i} A_{ij} z_{ji} = 0; \tag{28b}$$

3) For $i \in \mathcal{N}$ and $j \in \mathcal{N}_i$, μ_i evolves as

$$\mu_i^{k+1} := \mu_i^k + \sum_{j \in \mathcal{V}_i} A_{ij} z_{ji}^{k+1} \tag{28c}$$

4) For $j \in \mathcal{N}_i$, λ_{ji} evolves as

$$\lambda_{ji}^{k+1} := \lambda_{ji}^k + d_{ji}^k \Big[x_j^{k+1} - z_{ji}^{k+1} \Big]. \tag{28d}$$

where μ_i is the dual variable used to relax the constraint (20b) in the z-minimization step [41]. The x-minimization step can be solved iteratively while the other steps have an explicit solution [36]. Under assumption 2, the ith agent can solve the x-minimization sub-problem using the gradient descent technique, that is

$$x_i^{k+1} = x_i^k - \alpha_i \left[\nabla_{x_i} f_i(x_i^k) + \sum_{j \in \mathcal{V}_i} d_{ij}^k \Big[\lambda_{ij}^k + (x_i^k - z_{ij}^{k-}) \Big] \right] \tag{29a}$$

where k is the time step and $\alpha_i > 0$ is the step size. The variable z_{ij}^{k-} is a previous solution of z-minimization step and is held constant until x_i^{k+1} reaches optimal solution. For x-minimization step, agent i gathers z_{ij}, λ_{ij} $(j \in \mathcal{V}_i)$ information through the communication network from its neighbors. Then z_{ji} has a closed form solution using the updated x_i as follows

$$z_{ji}^{k+1} = x_j^{k+1} + \frac{1}{d_{ji}^k} \Big[d_{ij}^k \lambda_{ji}^k - A_{ij}^T \mu_i^k \Big], \tag{29b}$$

For z-minimization step, agent i obtains x_j, d_{ji} $(j \in \mathcal{N}_i)$ form its neighbors. Finally, the dual updates are given as follows

$$\mu_i^{k+1} = \mu_i^k + \sum_{j \in \mathcal{V}_i} A_{ij} z_{ji}^{k+1}, \tag{29c}$$

$$\lambda_{ji}^{k+1} = \lambda_{ji}^k + d_{ji}^k \Big[x_j^{k+1} - z_{ji}^{k+1} \Big]. \tag{29d}$$

The dynamic update laws defined in (29) is a gradient-based optimization, and assuming assumption 2 holds, the trajectory generated by the primal and dual variables moves closer to the optimal solution. The primal variables generate a trajectory towards the negative direction of the gradient and the dual variables produce trajectory in the positive direction of the gradient. From (29a), the amount of distance covered by the trajectory towards optimality in each iteration can be calculated as follows:

$$x_i^{k+1} - x_i^k = -\alpha_i \left[\nabla_{x_i} f_i(x_i^k) + \sum_{j \in \mathcal{V}_i} d_{ij}^k \Big[\lambda_{ij}^k + (x_i^k - z_{ij}^{k-}) \Big] \right]$$

If we divide both side by a small number Δt, we get

$$\frac{x_i^{k+1} - x_i^k}{\Delta t} = -\alpha_i^{'} \Big[\nabla_{x_i} f_i(x_i^k) + \sum_{j \in \mathcal{V}_i} d_{ij}^k \Big[\lambda_{ij}^k + (x_i^k - z_{ij}^{k-}) \Big] \Big]$$

where $\alpha_i^{'} = \frac{\alpha_i}{\Delta t}$. By taking the limit, we can approximate the discrete time steps into the continuous domain. For x update, we have

$$\begin{aligned} \lim_{\Delta t \to 0} \frac{x_i^{k+1} - x_i^k}{\Delta t} &= \dot{x}_i \\ &= -\alpha_i^{'} \left[\nabla_{x_i} f_i(x_i) + \sum_{j \in \mathcal{V}_i} d_{ij} \Big[\lambda_{ij} + (x_i - z_{ij}^{-}) \Big] \right] \end{aligned} \tag{30}$$

Following similar procedure for z, λ and μ, we obtain the equations provided in theorem 1. ■

B. Proof of Lemma 1

Let us consider $x_i^*, z_{ji}^*, \lambda_{ji}^*$ and μ_i^* as the primal-dual optimizer of (22) which satisfies the KKT conditions [42]. Thus, we can define the error states as $\tilde{x}_i = x_i - x_i^*$, $\tilde{z}_{ij} = z_{ij} - z_{ij}^*$, $\tilde{\mu}_{ij} = \mu_{ij} - \mu_{ij}^*$ and $\tilde{\lambda}_{ij} = \lambda_{ij} - \lambda_{ij}^*$ and redefine the update law as:

$$\dot{\tilde{x}}_i = -\alpha_i^{'} \left[\eta_i(x_i, x_i^*) + \sum_{j \in \mathcal{V}_i} d_{ij} \Big[\tilde{\lambda}_{ij} + (\tilde{x}_i - \tilde{z}_{ij}^{-}) \Big] \right] \tag{31a}$$

$$\dot{\tilde{z}}_{ji} = \alpha_i^{'} [d_{ji} \tilde{\lambda}_{ji} + d_{ji}(\tilde{x}_j - \tilde{z}_{ji}) + A_{ij}^T \tilde{\mu}_i] \tag{31b}$$

$$\dot{\tilde{\mu}}_i = \sum_{j \in \mathcal{V}_i} A_{ij} \tilde{z}_{ji} \tag{31c}$$

$$\dot{\tilde{\lambda}}_{ji} = d_{ji}(\tilde{x}_j - \tilde{z}_{ji}). \tag{31d}$$

where $\eta_i(x_i, x_i^*) = \nabla_{x_i} f_i(x_i) - \nabla_{x_i^*} f_i(x_i^*)$. Consider the Lyapunov function

$$\begin{aligned} V = \sum_{i=1}^{N} \frac{1}{2\alpha_i^{'}} \Bigg\{ &||\tilde{x}_i||^2 + \alpha_i^{'} ||\tilde{\mu}_i||^2 + \sum_{j \in \mathcal{V}_i} ||\tilde{z}_{ij}||^2 + \alpha_i^{'} ||\tilde{\lambda}_{ij}||^2 \\ &+ \alpha_i d_{ij} \int_{t-\delta}^{t} ||\tilde{z}_{ij}(\tau)||^2 d\tau \Bigg\} \end{aligned}$$

Taking the time-derivative of V yields

$$\begin{aligned} \dot{V} = \sum_{i=1}^{N} \Bigg\{ &- \eta_i(x_i, x_i^*) + \tilde{\mu}_i^T \sum_{j \in \mathcal{V}_i} A_{ij} \tilde{z}_{ji} \\ &+ \sum_{j \in \mathcal{V}_i} \Bigg[\tilde{x}_i^T \Big[- d_{ij} \tilde{\lambda}_{ij} - d_{ij}(\tilde{x}_i - \tilde{z}_{ij}^{-}) \Big] \\ &+ \tilde{z}_{ij}^T \Big[d_{ij} \tilde{\lambda}_{ij} + d_{ij}(\tilde{x}_i - \tilde{z}_{ij}) - A_{ij}^T \tilde{\mu}_i \Big] \\ &+ d_{ij} \tilde{\lambda}_{ij}^T \Big[\tilde{x}_i - \tilde{z}_{ij} \Big] + \frac{1}{2} d_{ij} ||\tilde{z}_{ij}||^2 - \frac{1}{2} d_{ij} ||\tilde{z}_{ij}^{-}||^2 \Bigg] \Bigg\} \end{aligned}$$

$\eta_i(x_i, x_i^*)$ is positive definite with respect to $\tilde{x}_i$ according to the global under-estimator property of the convex function. Hence we have

$$\begin{aligned}\dot{V} =& \sum_{i=1}^{N}\Bigg\{ -\eta_i(x_i,x_i^*) + \sum_{j\in\mathcal{V}_i}\Bigg[-d_{ij}\tilde{x}_i^T\tilde{x}_i + d_{ij}\tilde{x}_i^T\tilde{z}_{ij}^- \\ & + d_{ij}\tilde{z}_{ij}^T\tilde{x}_i - \frac{1}{2}d_{ij}\tilde{z}_{ij}^T\tilde{z}_{ij} - \frac{1}{2}d_{ij}||\tilde{z}_{ij}||^2\Bigg]\Bigg\}. \\ =& \sum_{i=1}^{N}\Bigg\{ -\eta_i(x_i,x_i^*) + \sum_{j\in\mathcal{V}_i}\Bigg[\frac{d_{ij}}{2}||\tilde{x}_i - \tilde{z}_{ij}||^2 \\ & + \frac{d_{ij}}{2}||\tilde{x}_i - \tilde{z}_{ij}^-||^2\Bigg]\Bigg\}.\end{aligned}$$

which is negative semi-definite with respect to all the variables and is negative definite with respect to $\tilde{x}_i$ as well as both $(\tilde{x}_i - \tilde{z}_{ij})$ and $(\tilde{x}_i - \tilde{z}_{ij}^-)$. ■